ELSEVIER

Journal of Biomechanics 40 (2007) 861–870

JOURNAL OF BIOMECHANICS

www.elsevier.com/locate/jbiomech
www.JBiomech.com

Snoring source identification and snoring noise prediction

Z.S. Liu[a,*], X.Y. Luo[b], H.P. Lee[a,c], C. Lu[a]

[a]*Institute of High Performance Computing, 1 Science Park Road, #01-01 The Capricorn, Singapore Science Park II, Singapore 117528, Singapore*
[b]*Department of Mathematics, University of Glasgow, G12 8QW, UK*
[c]*Department of Mechanical Engineering, National University of Singapore, 9 Engineering Drive 1, Singapore 119260, Singapore*

Accepted 10 March 2006

Abstract

This paper investigates the snoring mechanism of humans by applying the concept of structural intensity to a three-dimensional (3D) finite element model of a human head, which includes: the upper part of the head, neck, soft palate, hard palate, tongue, nasal cavity and the surrounding walls of the pharynx. Results show that for 20, 40 and 60 Hz pressure loads, tissue vibration is mainly in the areas of the soft palate, the tongue and the nasal cavity. For predicting the snoring noise level, a 3D boundary element cavity model of the upper airway in the nasal cavity is generated. The snoring noise level is predicted for a prescribed airflow loading, and its range agrees with published measurements. These models may be further developed to study the various snoring mechanisms for different groups of patients.

Keywords: Finite element method; Boundary element method; Vibration; Snoring noise; Soft palate; Tongue; Nasal cavity; Human head model; Structural intensity

1. Introduction

Snoring is defined as the sounds made by vibrations in the soft palate and their adjacent tissues (such as the posterior faucial pillars) during sleep. Researchers have shown that it is the most important symptom connected with the obstructive sleep apnea (OSA) syndrome, as well as the cause of much disruption to bed partners and to the snorer (Verin et al., 2002). Current research also shows that snoring might indicate the first stage of the OSA syndrome (Lugaresi et al., 1978). Heavy snoring can result in sleep-related upper airway narrowing, which leads to respiratory flow limitation and increased respiratory effort. Strong inspiratory suction may, secondarily, cause a total upper airway collapse. If untreated, heavy snoring may be complicated by excessive daytime sleepiness. Hence, snoring has received much clinical attention in recent years. These studies are mainly devoted to the effects of snoring on health and to the treatment effects (Aurégan and Depollier, 1995; Ayappa and Rapoport, 2003). To our knowledge, only limited research work has been carried out to understand the mechanisms of snoring and to control it.

Using signal-averaged anatomic data from male and female subjects, Malhotra et al. (2002) developed representative male and female finite element (FE) airway models at the Harvard medical school. However, their FE analysis is only for a two-dimensional (2D) model of the upper airway. Beck et al. (1995) presented the study of clarifying the acoustic properties of snores by using an experimental setup in the time and frequency domains. They found that snoring sounds can be characterized by repetitive sequences of sound structures, which contain large low-frequency waveforms interwoven with rapid oscillation. They identified two dominant patterns, from their analysis of the

*Corresponding author. Tel.: +65 64191289; fax: +65 64191280.
E-mail addresses: liuzs@ihpc.a-star.edu.sg (Z.S. Liu), x.y.luo@maths.gla.ac.uk (X.Y. Luo), hplee@ihpc.a-star.edu.sg (H.P. Lee), luchun@ihpc.a-star.edu.sg (C. Lu).

0021-9290/$ - see front matter © 2006 Elsevier Ltd. All rights reserved.
doi:10.1016/j.jbiomech.2006.03.022

snores, which are distinctly different from each other: one is the "simple-waveform" and the other is the "complex-waveform." Although the acoustic properties were presented, the mechanism of inducing snoring and the method to control it were not presented. Wilson et al. (1999) investigated the snoring sound intensity levels generated by individuals during polysomnographic testing and explored the associations between snoring sound intensity and a variety of demographic and clinical factors. They reported that a greater sound intensity appeared to be the result of greater negative pressures on resumption of breathing in apneic snorers, resulting in high flow rates, turbulent flow and greater forces on the vibrating structures. Aittokallio et al. (2001) presented a mathematical model to predict the nasal flow profile from three critical components that control the upper airway patency during sleep. Some mathematical models of the upper airway as a collapsible tube have been developed to study snoring. Gavriely and Jensen (1993) studied a simple theoretical model of the upper airways, consisting of a movable wall in a channel segment that was connected to the airway opening via a conduit with a resistance. The upper airway narrowing, collapsibility, and resistance were recognized as predisposing factors for snoring and obstructive sleep apnea. Liistro et al. (1999) studied the influence of gas density on simulated snoring production and supraglottic resistance through a theoretical model of the upper airway which was related to instability of the upper airway. They demonstrated that the snoring occurred at lower flow rates when gas density was increased. Huang (1995) modeled the mechanics of the soft palate during oronasal snoring by carrying out a linear stability analysis on a 2D flow over an elastic plate. Luo and Pedley (1996, 2000) studied the system behavior of steady and unsteady flow in a collapsible channel, which was useful in understanding the mechanisms of self-excited oscillations in such a system. However, due to the highly simplified nature of these models, to date our understanding of upper airway narrowing, collapsibility, and resistance and their interaction is still far from satisfactory and the mechanisms of snoring remain to be explored.

Although there have been some more detailed CFD models on nasal turbulence, the larynx, and vocal folds, there are either limited to 2D, or on particular part of the problem e.g. flow features only, and are not directly focused on snoring mechanisms in a whole human head and neck. Zhang and Kleinstreuer (2003) studied low Reynolds number turbulence flow in locally (rigid) constricted ducts, Gemci et al. (2002) studied inhalation in a three-dimensional (3D) simple rigid throat model, and Zhang et al. (2005) studied the snoring mechanism for a 2D flexible wall channel. However, all these models inevitably employed simplified geometric models to investigate certain physical mechanism. To the best of our knowledge, none of the published work has used a more detailed 3D geometry for a whole human head to study the snoring mechanism.

This study aims to investigate the snoring mechanism by developing a 3D FE model of the human head and neck which includes the whole upper airway. The model includes the upper part of the head, neck, soft palate, hard palate, tongue, nasal cavity and the surrounding walls of the pharynx. A novel application of the structural intensity (SI) methodology (Liu et al., 2004, 2005) is adopted to identify snoring characteristics by using the vibro-acoustic noise control concept. Here, SI is the power flow or energy flow per unit cross-sectional area in an elastic medium. It is analogous to the acoustic intensity due to structural vibration in a fluid medium. Since the SI field indicates the magnitude and direction of the vibrational energy flow at any point of the structure, it is useful to investigate the SI of the tissue structure in the throat from a vibration and noise control point of view. The SI distribution can offer complete information of energy transmission paths and positions of sources and sinks of the energy of vibration. Therefore, by changing the energy flow effectively within the upper airway and hence the amount of energy injected into the tissue structure, one may control the vibration of the soft tissues and the wall surface of the upper airway and hence the noise level of snoring.

One of the purposes of this paper is to investigate the snoring mechanism from a biomechanical point of view through a FE dynamic analysis of the human head. The snoring sources and sinks which may be used as snoring control or snoring treatment locations, will be identified by using the SI concept. The second objective of the present paper is to predict the snoring noise intensity level using the vibro-acoustic concept. Some simulation results including vibration modes, SI field and energy flow transmission which can indicate possible snoring source and sinks, as well as the snoring noise level will be given in the example. We hope this study can provide some useful information for further snoring noise control studies.

2. Finite element model of a human head

In order to investigate the snoring mechanism caused by the vibration of soft tissue structures, the whole human head is modeled by using solid and shell FEs as shown in Figs. 1 and 2. The FE model of the upper part of the human head is generated according to the ISB library (http://www.isbweb.org), while the remaining parts such as the soft palate, hard palate, tongue and nasal cavity are created manually according to anatomical section figures of the human head found in the literature (Crafts, 1985; Martini et al., 2000; Moore, 1992). In the FE model, the major structures of interest,

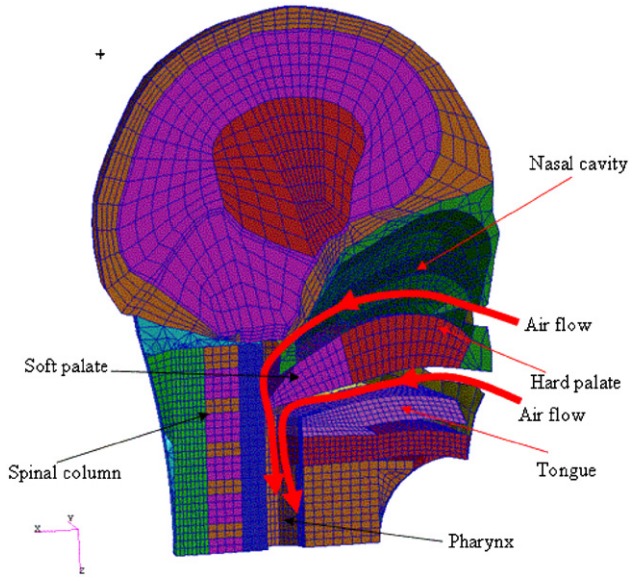

Fig. 1. Finite element (FE) model of a human head. The red arrows indicate the airflow paths in the cavity. Only half of the model is shown.

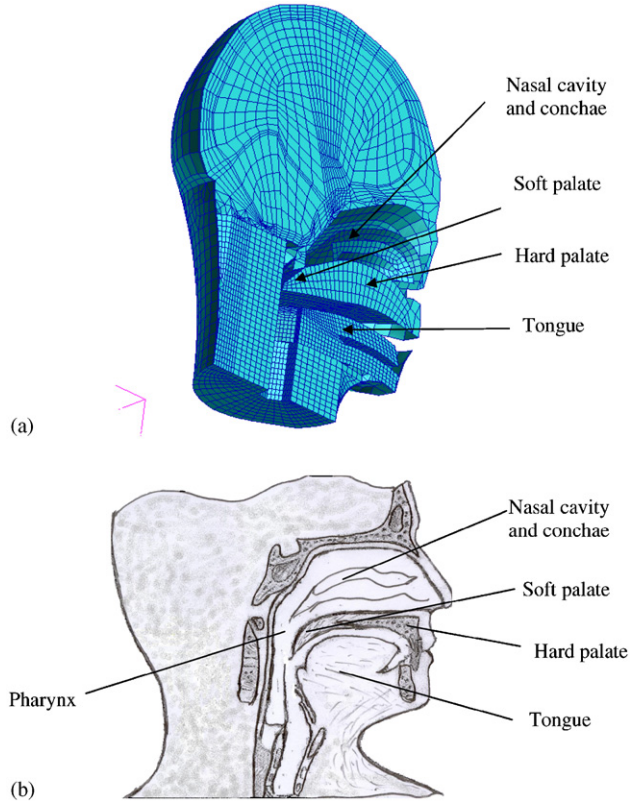

Fig. 2. Comparison of FE model with the anatomy drawing of human head section. (a) FE model, and (b) schematic diagram of anatomy section view of lower part of human head.

such as the soft palate, tongue and neck, are modeled using solid elements in order to more accurately represent the structured tissues. In the half FE model, the number of element and node are 24349 and 24119, respectively. It is demonstrated according to a sensitive study for different FE models with different elements number, that the present FE model is adequate to cover the major dynamic response phenomena for interesting parts such as the soft palate, tongue, nasal cavity, etc. Fig. 2 illustrates the typical representative prototype of a human head. Note that although every effort is made to replicate the main 3D features here, some geometric simplifications are necessary, e.g. the extrathoracic airway is not modeled in detail, and certain parts are simplified as solid or plate elements.

The material properties of the model assigned to upper different parts of the head are assumed to be isotropic, homogeneous and elastic (Willinger et al., 1999). The main vibration parts of the model such as the soft palate, hard palate, tongue, and cartilages are modeled as solid elements. As the tongue tissues are mainly composed of water, Poisson's ratio of the tongue is taken to be 0.49 in order to model the quasi-incompressibility. The Young's modulus of the tongue is chosen from Payan et al.'s work (Payan et al., 1998). For the soft palate, we assume that Young's modulus and Poisson's ratio are 25 kPa and 0.42, respectively (Malhotra et al., 2002; Huang et al., 1995; Huang and Williams, 1999). The material properties of the main parts of the head and neck are shown in Table 1.

In the dynamic response analysis, the tongue and the soft palate material are assumed to be viscoelastic materials. The mechanical behavior of the soft palate is considered to be nonlinear and viscoelastic (Wu et al., 2004a, b). The stress is assumed to be decomposed into an elastic stress, representing an instantaneous soft tissue response, and a viscous stress, representing a delayed tissue response. The constitutive relation can be expressed as (Wu et al., 2004a, b; Tschoegl, 1989)

$$\sigma(t) = \sigma_0(t) + \int_0^t \dot{g}(\tau)\sigma_0(t-\tau)\,\mathrm{d}\tau, \tag{1}$$

where t is time. The first term on the right-hand side of the equation is the elastic stress component and the second term represents viscous stress components. The viscoelastic behavior of the soft palate is modeled using a stress relaxation function based on the Prony series, there is

$$g(t) = \frac{G(t)}{G_0} = \left[1 - \sum_i^N g_i(1 - \mathrm{e}^{-(t/\tau_i)}\right], \tag{2}$$

where $G(t)$ and G_0 are the instantaneous and time-dependent modulus, respectively, g_i and τ_i $(i = 1, 2, \ldots, N)$ are stress relaxation parameters and N is the number of terms used in the stress relaxation function. The viscous parametric values (g_i, τ_i) used in the present dynamic response analysis are shown in Table 2 (Wu et al., 2004a, b). The effects of the internal dissipative forces

Table 1
Material properties of the human head and neck model used in the simulation

Material		Young's modulus E (MPa)	Poisson's ratio (v)	Density ρ (kg/m^3)
Skull	Outer table	7300	0.22	3000
	Diploe	3400	0.22	1744
	Inner table	7300	0.22	3000
CSF		2.19	0.489	1040
Brain		2190	0.4996	1040
Willinger_Face		5000	0.23	2500
Scalp		16.7	0.42	1130
Kleiven_Trabecular		1000	0.24	1300
Kleiven_Cortical		15000	0.22	2000
Falx_and_Tentorium		31.5	0.45	1140
Visco_brain		122999	0.499	1040
Hard palate		2	0.22	1040
Soft palate		0.025	0.42	1040
bone		7300	0.22	3000
tongue		0.015	0.499	1040
Bio_disk		7.584	0.35	1140
Bio_cord		2190	0.499	1040

Table 2
Viscoelastic parameters of soft palate used in the simulation

Number i	1	2
g_i	0.4621	0.4959
τ_i (s)	0.07294	9.610

of other parts are taken into account by assuming a 5% structural damping.

The soft palate is a very flexible structure located at the confluence of the nasal and buccal tracks where they are connected with the pharynx. The soft palate vibrates at a frequency of 20–80 Hz (Issa and Sullivan, 1984; Aurégan and Depollier, 1995), during snoring, and the airflow paths are shown in Fig. 1. The response frequencies are selected to be 20, 40 and 60 Hz, which are close to the natural frequencies of the soft palate and tongue structures.

3. Structural intensity (SI) and snoring noise

The instantaneous intensity component in the time domain can be defined according to Noiseux (1970), Pavic (1976), Liu et al. (2004, 2005, 2006) as

$$I_i(t) = -\sigma_{ij}(t)v_j(t), \quad i,j = 1,2,3. \tag{3}$$

For a steady-state vibration, the active SI in the frequency domain can be defined as

$$I_i(\omega) = -(1/2)\,\mathrm{Re}(\tilde{\sigma}_{ij}(\omega)\tilde{v}_j^*(\omega)), \quad i,j = 1,2,3, \tag{4}$$

where $\tilde{\sigma}_{ij}(\omega)$ is the complex amplitude of the Fourier transform of the stress $\sigma_{ij}(t)$ tensor and $\tilde{v}_j^*(\omega)$ is the complex conjugate of the Fourier transform of the velocity $v_j(t)$ tensor.

As the SI is a vector field in 3D space, it is similar to a velocity field in a fluid flow. Inspired by the streamline concept in fluid mechanics, we use the SI streamline representation to interpret the SI transmission paths (Liu et al., 2005, 2006). Similar to the fluid mechanics definition, the SI streamline can be expressed as

$$d\mathbf{r} \times \mathbf{I}(\mathbf{r}, t) = 0, \tag{5}$$

where $\mathbf{r}$ is energy flow particle position, $\mathbf{I}$ is the vector form of SI. The SI of an energy flow element on such a streamline is perpendicular to $\mathbf{r}$ and parallel to $d\mathbf{r}$. Therefore, the source and sink of the structural energy can be determined.

The stresses and velocities of the human head under an airflow pressure load are determined from structural frequency dynamic analysis, from which the structure intensity can be calculated according to Eq. (4). The commercial software ABAQUS (2003) is used to obtain the simulated harmonic vibration response.

In order to predict the snoring noise level that is generated by the vibration of the tissues, mouth and nose cavities, a boundary element (BE) model representing the vibration surface of the upper airway cavity is generated from the FE model (as shown in Fig. 3). In the BE model, the cavity surfaces which include the whole upper airway are assumed to be in vibration (Wilhelms-Tricarico, 1996), as the air flows into the cavity, noise is generated. The noise level in the objective plane, defined to be in front of the human face just near the mouth and nose, which contains 36 field points, will be predicted.

The starting point of the BE formulation is the Helmholtz integral equation, which relates the surface integral of the acoustic parameters over the surface of the body of interest to the acoustic field outside the body (Liu et al., 2004, 2006). The noise level which is

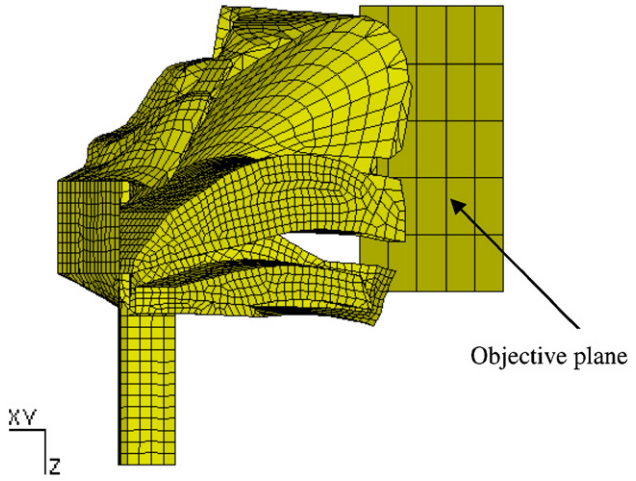

Fig. 3. Boundary element (BE) model of cavity surface for snoring noise simulation (only half of the model is shown), and the objective plane.

generated by soft tissue vibration can be computed by using the BE method. In the noise analysis, the cavity surface vibrating displacements/velocities in human upper airway are determined first from a vibration frequency response analysis. Then, these vibration displacements/velocities which form the BE boundary conditions, are projected to the cavity surfaces (Fig. 3).

In the acoustic BE indirect method, the system equations can be written as follow (Coyette 1999):

$$\begin{bmatrix} B & C^{\mathrm{T}} \\ C & D \end{bmatrix} \begin{Bmatrix} \lambda \\ \mu \end{Bmatrix} = \begin{Bmatrix} f \\ g \end{Bmatrix}, \tag{6}$$

where the matrixes B, C and D are influence matrices which are symmetric and frequency dependent, λ is vector of jump of velocity, and μ is the vector of jump of pressure. f and g are excitation vectors. The sound pressure and intensity of arbitrary field point $\mathbf{x}$ can be determined from the surface results. Consider a cavity bounded by a surface S, the acoustic pressure at an outside field point $\mathbf{x}$ can be obtained by using a boundary jump in velocity and a jump of pressure and the Helmholtz integral formula takes the form

$$p(x) = \int_S \left[\mu(y) \frac{\partial G(x,y)}{\partial n_y} - \lambda(y) G(x,y) \right] \mathrm{d}S(y), \tag{7}$$

where p is the acoustic pressure potential satisfying the Helmholtz differential equation $\nabla^2 p + k^2 p = 0$ for time harmonic waves present in the acoustic medium Ω inside the airway and nasal cavity. G is Green's function (fundamental solution of the Helmholtz equation for a point source), $G(\mathbf{x},\mathbf{y}) = \exp[-ik\mathbf{r}(\mathbf{x},\mathbf{y})]/\mathbf{r}(\mathbf{x},\mathbf{y})$ in which $\mathbf{r}(\mathbf{x},\mathbf{y})$ describes the distance between any point $\mathbf{y}$ on S and any field point $\mathbf{x}$, $k = \omega/c$ is the wave number, ω is the circular frequency and c is the velocity of air, n_y is the outward unit normal of S at $\mathbf{y}$. According to this principle, the snoring noise level at the prescribed objective points can be calculated. In this prediction, the commercial software SYSNOISE (2004) is adopted for noise prediction in the objective plan.

4. Results

In order to identify the characteristics of snoring from the human head, the modal analysis is carried out first. Normal mode analysis can provide the relative deformation of all parts under each natural frequency (i.e. the modes). It was found from this analysis that the main deformation in the mode shapes of the whole head for a frequency range of 10–60 Hz are most concentrated on the nasal cavity, soft palate and tongue areas. Fig. 4 shows the mode shapes at the natural frequencies 14.4, 22.4, 22.6, 44.5, 46.9 and 57.7 Hz. It can be observed from Fig. 4 that the main deformation in the mode shapes, are shifted from the nasal cavity to the soft palate and to the tongue, and from the tongue to the soft palate and to the nasal cavity as the frequency changes, indicating different sensitive regions for a different excitation frequency. At the lowest frequency of 14.4 Hz, the deformations of the nasal cavity and the soft palate have the same and the largest deformation level. The end of the soft palate is the most sensitive part at the frequency of 22.4 Hz. The largest response moves to the tongue when the frequency increases to 22.6 Hz. Both the soft palate, and the back of the nasal cavity become more sensitive for a higher frequency of 44.5, this is to be more or less the same for 46.9 Hz. Finally, at an even higher frequency of 57.7 Hz, the hard palate, soft palate, and the whole nasal cavity start to be important, and the mode becomes more spread out. It is interesting to note that the tongue is only sensitive at 22.6 Hz, while the soft palate is sensitive throughout the whole frequency range (except at 22.6 Hz when the tongue becomes dominate), indicating its importance in the snoring mechanism. In general, these observations agree with the clinical observation that human snoring normally takes place at a pressure of 20–80 Hz (Issa and Sullivan, 1984; Aurégan and Depollier, 1995).

A frequency response analysis is then performed for the frequency range of 20–60 Hz. In the dynamic frequency response analysis, the airflow pressure load is assumed to be sinusoidal shape with amplitude of 1500 Pa (Aurégan and Depollier, 1995; Malhotra et al., 2002; Huang et al., 1995; Huang and Williams, 1999, Woodson et al., 1997; Amis et al., 1999). This represents the average pressure load under a normal breathing pattern which is usually estimated to be between 1127.8 and 1667.0 Pa (Malhotra et al., 2002). The pressure is applied to free surface in the cavities. Fig. 5 depicts the deformation contours for 20, 40, 60 Hz, respectively. It is seen from the figures that for 20 Hz pressure load the vibrations of soft tissues of the upper airway are mainly

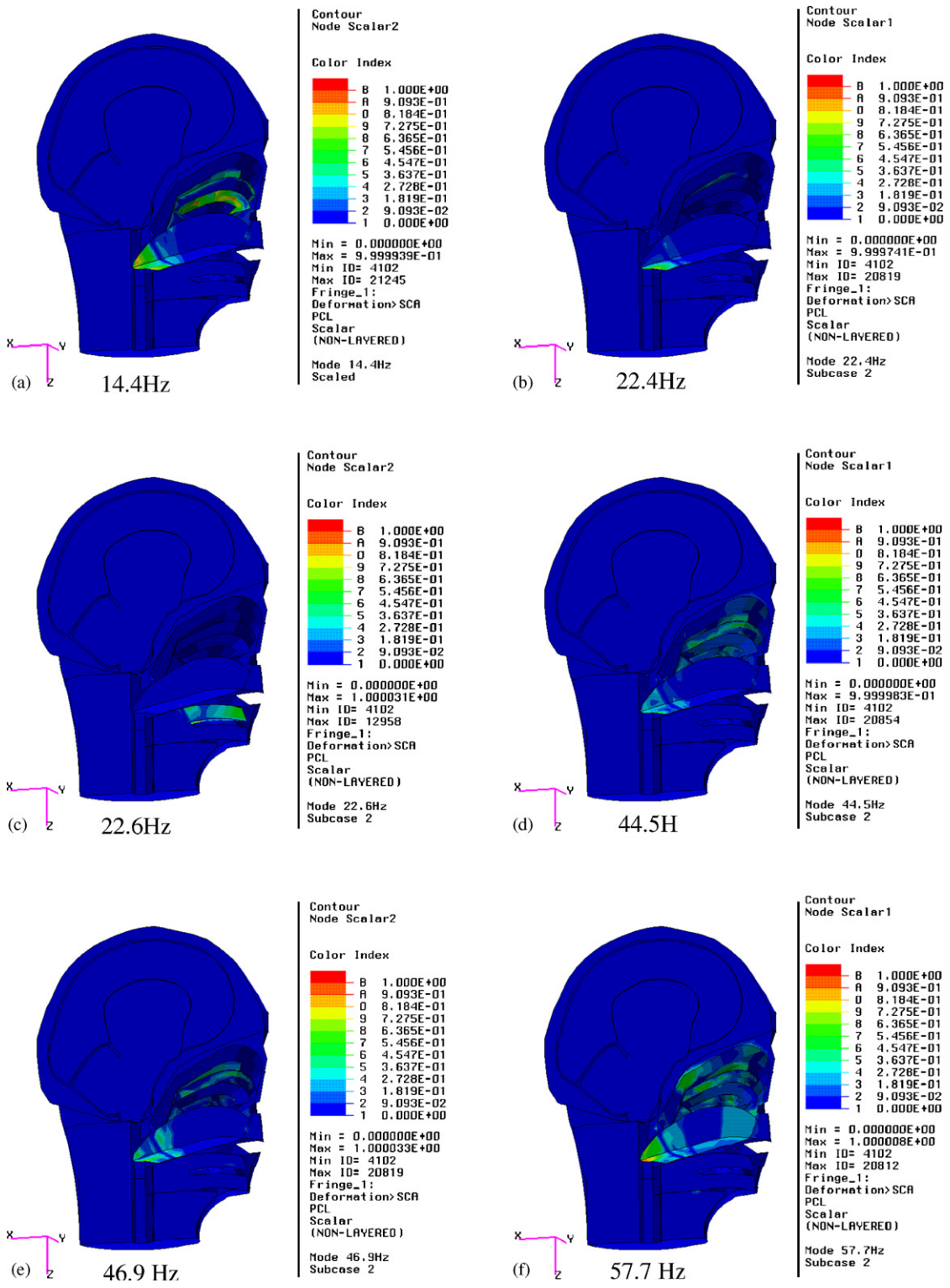

Fig. 4. Mode shapes of the human head model at different natural frequencies (the contour color index is scaled between 0 and 1). (a) 14.4 Hz, (b) 22.4 Hz, (c) 22.6 Hz, (d) 44.5 Hz, (e) 46.9 Hz, and (f) 57.7 Hz.

in the areas of the soft palate and tongue. While for the 40 Hz response, the deformation is concentrated on the soft palate areas. For the 60 Hz response, the deformations are found to extend to soft palate, tongue and nasal cavity areas. This is consistent with the results of the modal analysis. To identify the snoring sources and sinks, the SI distributions at 20, 40 and 60 Hz are shown in vector form in Fig. 6. The energy flow of the human

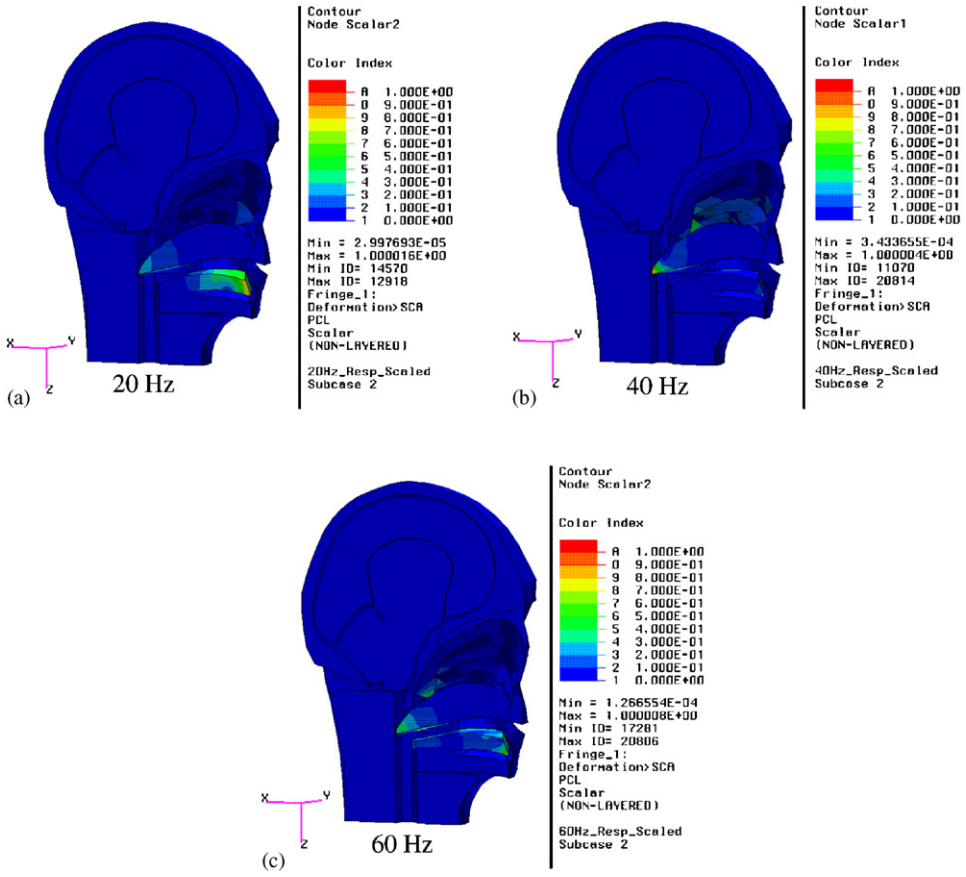

Fig. 5. Displacement contours of the human head model from frequency dynamic responses at pressure load cases (the contour color index is scaled between 0 and 1): (a) 20 Hz, (b) 40 Hz, and (c) 60 Hz.

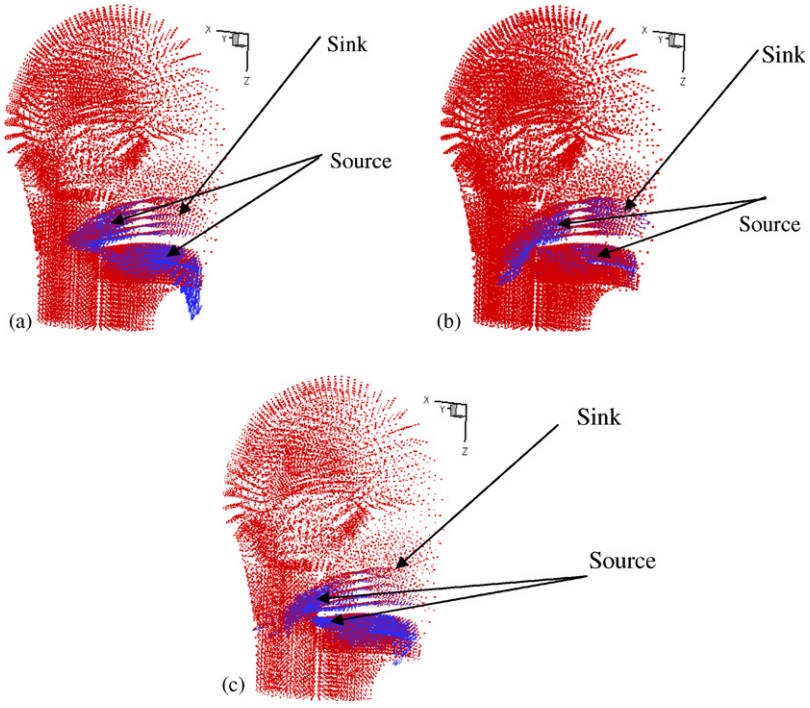

Fig. 6. Structural intensity (SI) vector distributions of the human head model from frequency dynamic responses at pressure load cases. The coordinates of the finite element nodal positions are shown in red, and SI vectors are shown in blue. The sources and sinks of the SI field are indicated by the arrows: (a) 20 Hz (scale factor 0.0035), (b) 40 Hz (scale factor 0.005), (c) 60 Hz (scale factor 0.0015).

head under an airflow pressure loading can be clearly identified from this figure. In order to clearly depict the SI vector, different scale factors are used for different frequencies. It can be demonstrated from Fig. 5 that the 60 Hz flow pressure is more sensitive to snoring vibration compared with the 20 and 40 Hz response. The sources and sinks of the SI distribution are indicated by the arrows in Fig. 6. It is shown that the sources are located at the soft palate end and tongue tip, while the sink is around the top of the hard palate towards the cavity. These highlight the key locations for further possible passive and/or active snoring control. In other words, the method, when applied to a detailed patient-specific head model, may provide important information for doctors to identify implement positions for the snoring treatments.

To obtain a quantitative estimation, the snoring noise level is calculated from surface vibration of the soft tissue of the upper airway. Snoring noise contours are shown in Fig. 7 for 20, 40 and 60 Hz frequencies. It can be seen that the noise level near the mouth and nose is much higher and the noise pressure is concentrated in the area in front of the mouth front. The average noise levels near the mouth and nose on the objective plane calculated from the noise pressure contours are approximately 71, 66 and 78 dBA for 20, 40 and 60 Hz response, respectively. The predicted noise level of snoring is in agreement with the measured results by Perez-Padilla et al. (1993) and Wilson et al. (1999). Wilson et al. (1999) showed that the snoring sound intensity is in the range of 50–70 dBA for 48% of the snoring patients in their study.

5. Discussion

A 3D FE human head model has been described for studying snoring noise. The model incorporates a number of new features compared with snoring models that have appeared in reported studies. Firstly, the present model incorporates not only the upper airway, but the whole head with realistic material properties for the head structure. Secondly, a novel SI approach is used to identify the energy source and sink. The model analysis is carried out first, and the noise level is evaluated from surface vibrations using the BE method. Thus detailed deformation and vibration of all parts within the head can be investigated. It is demonstrated,

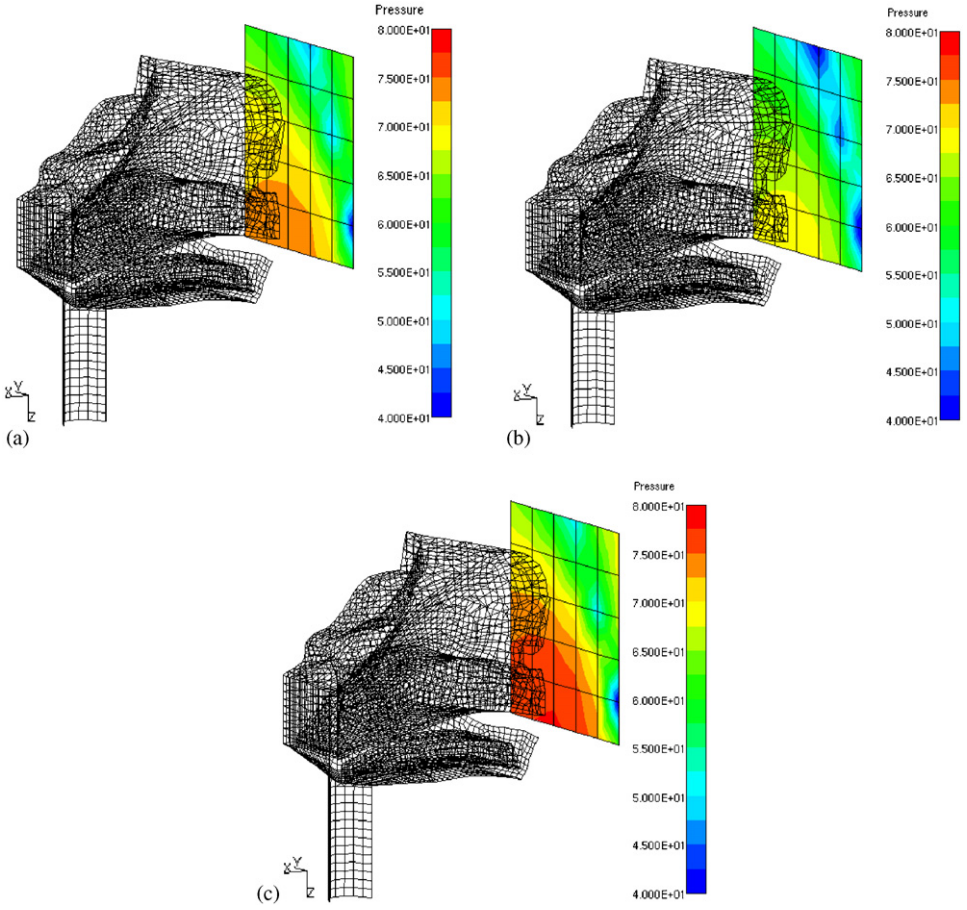

Fig. 7. Noise contours on the objective plane from human snoring at different frequencies.

by building this model what the most sensitive (vibrating parts) of the soft tissues in the head are under certain excitation frequencies. The sources and sinks of the SI are found to be closely related to these parts. These characteristics are extremely helpful to clinicians to identify and/or control the patient snoring. It is noted that our model is still simplified, and is only representative for a healthy human's anatomy, however, the methodology can be applied for a patient specific model to account for any effects of abnormal structure on snoring levels.

The limitations of the current work are discussed in the following:

The pressure waveform applied to the structure is assumed to be a uniform distributed pressure dynamic load with a sinusoidal waveform as detailed fluid–structure interactions (FSIs) are not modeled. This will differ somewhat to a detailed FSI which is again structure (detailed geometry) dependent and highly complicated, but is essential for this study since we are investigating the structure response to various frequencies, and not a patient specific dynamic response at this stage. However, once we have this information, detailed FSI information is only going to change the proportion of the pressure amplitude at each of the frequencies, and will not change the structure's sensitivities on certain dominant frequencies, which is what we have identified here.

The 3D geometry itself is still greatly simplified compared to a patient specific model. For example, extrathoracic airways are not modeled, and geometries of the hard palate, soft palate, and tongue are simplified. Also, the coupling interactions of airflow and soft tissues are not considered at this stage due to complexity reasons. As a result, the upper airway cannot collapse due to snoring, which is also considered to be one of the important mechanisms (Aittokallio et al., 2001). The coupling effect on snoring noise prediction would be meaningful for further study of snoring noise prediction. Also, the airflow pressure and frequency are all patient dependent and will need to be determined individually for a patient specific model.

In future work, other details such as extrathoracic airways and FSI will be considered, to improve the model. However, we have demonstrated that, with a simplified, representative prototype, the SI concept can be used to provide a useful tool for further study, and the model can be extended/developed with applications to passive/active snoring control and patient-specific medical treatments.

6. Concluding remarks

A 3D FE model of the human head and neck, which represents more realistic human upper airways compared to previous studies, is developed. It has been demonstrated that the SI approach is a useful method to identify the vibro-acoustic snoring noise source and the most sensitive tissue parts for a given pressure load. Furthermore, the upper airway BE cavity model for the snoring intensity study is developed. The snoring noise level based on the surface vibration is also predicted using the BE method for a given air flow pressure. The predicted noise level is in agreement with some measured data that are published previously. This model may be extended to explore various snoring mechanisms, as well as to provide a design tool in the active/passive snoring noise control, and patient-specific medical treatments.

Acknowledgments

The authors are grateful to the UK Royal Society of London for providing the Incoming Short Visit Award to the first author, which initiated this collaborative work.

References

ABAQUS, 2003. Analysis User's Manual 6.4. ABAQUS, Inc.

Aittokallio, T., Gyllenberg, M., Polo, O., 2001. A model of a Snorer's upper airway. Mathematical Biosciences 170 (1), 79–90.

Amis, T.C., O'Neill, N., Wheatley, J.R., van der Touw, T., di Somma, E., Brancatisano, A., 1999. Soft palate muscle responses to negative upper airway pressure. Journal of Applied Physiology 86, 523–530.

Aurégan, Y., Depollier, C., 1995. Snoring: linear stability analysis and in-vitro experiments. Journal of Sound and Vibration 188, 39–53.

Ayappa, I., Rapoport, D.M., 2003. The upper airway in sleep: physiology of the Pharynx. Sleep Medicine Reviews 7 (1), 9–33.

Beck, R., Odeh, M., Oliven, A., Gavriely, N., 1995. The acoustic properties of snores. European Respiratory Journal 8 (12), 2120–2128.

Coyette, J.P., 1999. The use of finite-element and boundary-element models for predicting the vibro-acoustic behavior of layered structures. Advances in Engineering Software 30 (2), 133–139.

Crafts, R.C., 1985. A Textbook of Human Anatomy, third ed. Churchill Livingstone Inc., New York.

Gavriely, N., Jensen, O., 1993. Theory and measurements of snores. Journal of Applied Physiology 74 (6), 2828–2837.

Gemci, T., Corcoran, T.E., Chigier, N., 2002. A numerical and experimental study of spray dynamics in a simple throat model. Aerosol Science and Technology 36 (1), 18–38.

Huang, L., 1995. Mechanical modeling of palatal snoring. Journal of the Acoustical Society of America 97 (6), 3642–3648.

Huang, L., Williams, J.E.F., 1999. Neuromechanical interaction in human snoring and upper airway obstruction. Applied Physiology 86, 1759–1763.

Huang, L., Quinn, S.J., Ellis, P.D.M., Williams, J.E.F., 1995. Biomechanics of snoring. Endeavour 19, 96–100.

http://www.isbweb.org/.

Issa, F.G., Sullivan, C.E., 1984. Upper airway closing pressure in snorers. Journal of Applied Physiology 43, 417–424.

Liistro, G., Veriter, C., Stanescu, D., 1999. Influence of gas density on simulated snoring. European Respiratory Journal 13 (3), 679–681.

Liu, Z.S., Lee, H.P., Lu, C., 2004. Active control of interior noise of box structure using structural intensity method. In: Proceedings of the 33rd International Congress and Exposition on Noise Control Engineering, Prague, Czech Republic, August 2004, pp. 22–25.

Liu, Z.S., Lee, H.P., Lu, C., 2005. Structural intensity study of plates under low velocity impact. International Journal of Impact Engineering 31 (8), 957–975.

Liu, Z.S., Lee, H.P., Lu, C., 2006. Passive and active interior noise control of box structure using structural intensity method. Applied Acoustics 67 (2), 112–134.

Lugaresi, E., Coccagna, G., Mantovani, M., 1978. Hypersomnia and periodic apneas. In: , Advances in Sleep Research, vol. 4. Spectrum Publications, Jamaica, NY, pp. 1–151.

Luo, X.Y., Pedley, T.J., 1996. A numerical simulation of unsteady flow in a 2-D collapsible channel. Journal of Fluid Mechanics 314, 191–225.

Luo, X.Y., Pedley, T.J., 2000. Flow limitation and multiple solutions of flow in collapsible channel. Journal of Fluid Mechanics 420, 301–324.

Malhotra, A., Huang, Y., Fogel, R.B., Pillar, G., Edwards, J.K., Kikinis, R., Loring, S.H., White, D.P., 2002. The male predisposition to pharyngeal collapse: the importance of airway length. American Journal of Research Critical Care and Medicine 166, 1388–1395.

Martini, F.H., Timmons, M.J., McKinley, M.P., 2000. Human Anatomy. Prentice-Hall International, Inc., London.

Moore, K.L., 1992. Clinical Oriented Anatomy. Williams & Wilkins, London.

Noiseux, D.U., 1970. Measurement of power flow in uniform beams and plates. Journal of the Acoustical Society of America 47, 238–247.

Pavic, G., 1976. Measurement of structure borne wave intensity, part I: formulation of the methods. Journal of Sound and Vibration 49 (2), 221–230.

Payan, Y., Bettega, G., Raphael, B., 1998. A biomechanical model of the human tongue and its clinical implication. MICCAI'98, LNCS 1496, Springer, Berlin, Heidelberg, pp. 688-695.

Perez-Padilla, J.R., Slawinski, E., Difrancesco, L.M., Feige, R.R., Remmers, J.E., Whitelaw, W.A., 1993. Characteristics of the snoring noise in patients with and without occlusive sleep apnea. American Review of Respiratory Disease 147 (3), 635–644.

SYSNOISE, Manual 5.6, LMS International, 2004.

Tschoegl, N.W., 1989. The Phenomenological Theory of Linear Viscoelastic Behavior: An Introduction. Springer, New York.

Verin, E., Tardif, C., Buffet, X., Marie, J.P., Lacoume, Y., Andrieu-Guitrancourt, J., Pasquis, P., 2002. Comparison between anatomy and resistance of upper airway in normal subjects, snorers and OSAS patients. Respiration Physiology 129, 335–343.

Wilhelms-Tricarico, R., 1996. A biomechanical and physiologically—based vocal tract model and its control. Journal of Phonetics 24 (1), 23–38.

Willinger, R., Kang, H.S., Diaw, B., 1999. Three-dimensional human head finite-element model validation against two experimental impacts. Annals of Biomedical Engineering 27 (3), 403–410.

Wilson, K., Stoohs, R.A., Mulrooney, T.F., Johnson, L.J., Guilleminault, C., Huang, Z., 1999. The snoring spectrum: acoustic assessment of snoring sound intensity in 1139 individuals undergoing polysomnography. Chest 115 (3), 762–770.

Woodson, B.T., Feroah, T.L., Connolly, A., Toohill, R.J., 1997. A method to evaluate upper airway mechanics following intervention in snorers. American Journal of Otolaryngology 18 (5), 306–314.

Wu, J.Z., Dong, R.G., Schopper, A.W., 2004. Modeling of time-dependent force response of fingertip to dynamic loading. Journal of Biomechanics 36 (3), 383–392.

Wu, J.Z., Dong, R.G., Schopper, A.W., 2004. Analysis of effects of friction on the deformation behavior of soft tissues in unconfined compression tests. Journal of Biomechanics 37 (1), 147–155.

Zhang, X., Ajaykumar, Z., Sudharsan, N.M., Kumar, K., 2005. Investigation of two-dimensional channel ow with a partially compliant wall using nite volume—nite di erence approach. International Journal of Numerical Methods in Fluids 49 (6), 635–655.

Zhang, Z., Kleinstreuer, C., 2003. Low-Reynolds-number turbulent flows in locally constricted conduits: a comparison study. AIAA Journal 41 (5), 831–840.